Rf

by Majeed Majeed

Effect of Embankment on The Behavior of Rigid Passive Pile Group in Sandy Soil

M. O. Karkush[1,a*], M. R. Sabaa[2,b], G. S. Jaffar[1,c], and O. K. Al-Kubaisi[3,d]

[1]Department of Civil Engineering, University of Baghdad, Baghdad, Iraq

[2]Al-Furat Al-Awsat Technical University, Al-Najaf, Iraq

[3]The School of Civil Engineering, the Faculty of Engineering, The University of Sydney, Darlington NSW 2006.

[a]mahdi_karkush@coeng.uobaghdad.edu.iq, [b]inm.mjd@atu.edu.iq, [c]ghofran_civi@yahoo.com, [d]omar.ismael@sydney.edu.au

Keywords: Passive pile; rigid pile group; embankment effect; sandy soil; model test.

Abstract. Piles can be damaged due to the lateral soil movement induced by constructing a nearby embankment. These movements introduce lateral loads "passive loads" on the piles which in turn increase the lateral forces and bending moments within the piles. In some cases, these induced forces and moments may exceed the pile capacity and cause failure. This research investigates experimentally the effects of soil movement on the behavior of nearby axially loaded and unloaded rigid pile groups driven in sandy soil having a dry unit weight of 13.5 kN/m^3. The model piles are made of aluminum and have an embedded length (Le) of 360 mm, free head of 140 mm, and diameter (D) of 10 mm. The embankment loads are applied at distances of 2.5D, 5D, and 10D from the edge of the pile group. The obtained results showed that the presence of axial loads decreases the displacement at the soil surface. It was found that the axially unloaded pile group (UG) had displaced more than the axially loaded pile group (LG) by 16, 25, and 35% at 2.5D, 5D, and 10D respectively. Moreover, increasing the distance between the embankment and the edge of the pile group had significantly decreased the maximum soil reaction due to the reduction of soil movement pressure.

Introduction

The construction of an embankment can impose excessive vertical loads on the soil underneath. These loads force the soil to move away from the loading source. This soil movement will apply lateral pressure on the front side of the pile which, in some cases, can exceed the pile capacity and cause failure. These lateral loads try to push the pile horizontally in the direction of loading which induces bending moment, rotation, and movement of the pile [1-2]. Based on the direction of load transfer between the pile and the surrounding soil, the laterally loaded pile can be classified into active piles or passive piles [3-5]. An active pile is mainly loaded at its top, with the lateral load being transferred to the soil such as the piles underneath the foundation of transmission towers and offshore structures. While a passive pile usually experiences lateral thrusts along its shaft arising from the horizontal movement of the surrounding soil such as piles used for slope stabilization and embankments [6]. Correct prediction of the displacements, moments, and shear forces caused by the moving soil can be considered as a key element in the design, construction, and serviceability of the type of piles [7]. Different factors have been found to affect the behavior of passive piles such as the material and geometric properties of piles, the profile of the moving soil, the axial loads, and the distance at which the pile is located from the boundaries of the moving soil.

The influence of a three-dimensional soil deformation on the response of a laterally loaded pile group in the sand has been investigated by conducting a series of model tests. The three-dimensional soil surface deformations around the piles had been obtained using a newly developed technique named Stereo-PIV [8]. Both Zhao et al. [9] and Zhang et al. [10] have presented a simplified analytical method to simulate the effects of soil movement due to soil excavation on the behavior of pile groups. They found that the lateral response of the passive pile groups obtained from the proposed method well agreed with those obtained from the centrifuge model tests. Furthermore, Ersoy and Yildirim

[11] have investigated the behavior of piles subjected to lateral soil movement imposed by slopes by conducting large-scale shear box experiments and the results have been compared with those found in the literature to enhance the understanding of the passive pile behavior.

In addition to that, Ibrahim and Hatem [12] have investigated the behavior of piles subjected to lateral soil movement in the sand. Different parameters have been utilized such as pile spacing, number of piles within a group, and pile head condition. The results showed that the maximum bending moment of pile groups has decreased as the pile spacing decreased and the pile has behaved as a single pile when the pile spacing has exceeded 7 times the diameter of the pile. Moreover, the influence of construction nearby embankment on the performance of existing single rigid and flexible piles inserted in sandy soil has been investigated [13-15]. The embankment load has been located at three different distances of 2.5D, 5D, and 10D from the edge of existing piles where D is the diameter of the pile. The results showed that the rigid pile with a shorter embedded length, Le = 360 mm, has provided more resistance to soil movement pressure. While Ren et al. [16] have conducted large geotechnical centrifuge model tests of two design schemes to simulate sheet-pile wharves with the load-relief platform in a homogeneous fine sand to evaluate the distribution of lateral pile-soil pressure and to distinguish between the pile's passive part and active part. On the other hand, Karkush and Kareem [17-18] have studied the behavior of passive piles in fine-grained textured soil contaminated with two ratios of petroleum products (MFO) under the effects of lateral soil movement. The results showed that as the percentage of soil contamination increased the impact of the embankment on the response of the passive piles has increased. In the present study, the response of the existing rigid pile group of (2×1) to the lateral soil movement induced by the construction of a nearby embankment has been investigated experimentally.

Material Properties

River sand can be classified as (SP-SM) according to the Unified Soil Classification System (USCS) has been used in this study. The mechanical properties of the soil have been evaluated based on ASTM and BS specifications [19-20]. The physical and mechanical properties of the soil have been listed in Table 1. A closed-end aluminum pipe of 500 mm long has been used in this study to model the pile. The mechanical properties of the aluminum model pile have been presented in Table 1. A slenderness ratio (L/D) of 50 and an embedded depth of 360 mm have been used in this study to ensure that the model pile behaves as a rigid pile according to the flexibility factor (K_R) shown in (Eq.1) in which E_p is the elasticity modulus of the pile; I_p is the moment of inertia of the pile; E_s is the secant modulus of the soil elasticity and L_e is the embedded length of the pile [21].

$$K_R = \frac{E_p I_p}{E_s L_e^4} < 10^{-5} \tag{1}$$

The model piles were instrumented with eight strain gauges, four of which have been located on the near side and the rest have been located on the far side of the model pile with respect to the embankment location, to measure the strain along the pile. The first pair of strain gauges have been located at the soil surface. A 60 mm spacing has been used between the first and the second pairs of strain gauges while 120 mm spacing has been used to distribute the rest as shown in Fig. 1a. The strain gauges have been numbered from SG1 to SG4 and each pair has been connected in a half Wheatstone bridge configuration as shown in Fig. 1b. The output voltage of the half-bridge configuration without including the temperature compensation can be expressed by (Eq. 2).

$$e_o = \frac{E}{2}\, K_s\, \varepsilon_o \tag{2}$$

where e_o is the output voltage; E is the bridge voltage; K_s is the gauge factor which is 2.12±1% in this study; and ε_o is the strain.

Table 1. Properties of the soil and the model pile.

Property of soil	Value	Property of soil	Value	Property of Pile	Value
Gs	2.67	γ_{dmin} (kN/m^3)	11.87	Outer diameter of pile (D)	10 mm
Cu	2.934	γ_{dmax} (kN/m^3)	15.14	Wall thickness of pile	1 mm
Cc	1.188	γ_d (kN/m^3) at Dr = 56%	13.5	Length of pile (L)	500 mm
Fines (%)	9.8	φ (°) at Dr = 56%	35°	Weight of pile	42 gm
Sand (%)	90.2	c (kPa)	9	Density of pile material	2.97 gm/cm^3
Dr (%)	56	Confined Modulus of Elasticity E_{oed} (kPa)	65770	Modulus of elasticity (Ep)	69.871 GPa

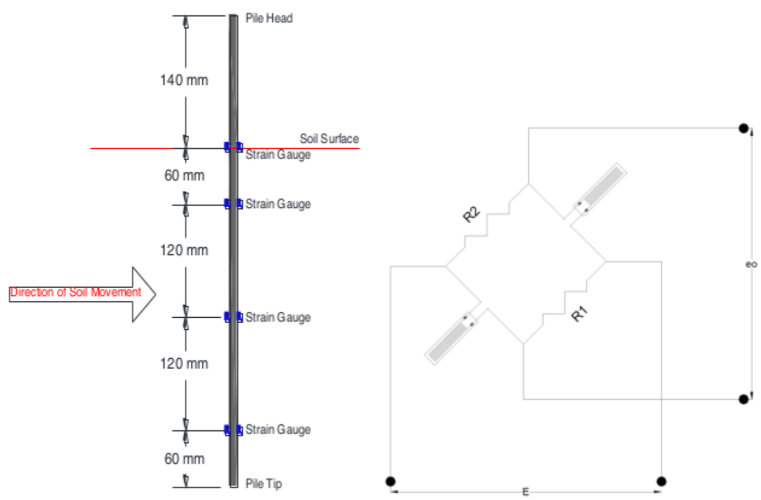

(a) (b)

Figure 1. Model pile details (a) strain gauges distribution (b) strain gauges configuration (half-bridge).

Experimental Settings and Testing Procedure

The experiments have been conducted in a steel container with dimensions of (800×800×800 mm). The raining technique has been used to pour the soil into the container from a specific height to achieve the required dry unit weight of 13.5 kN/m^3. To find the required height to achieve the required soil density, four pouring heights of 100, 200, 300, and 400 mm have been used to capture the effect of the pouring height on the soil density as shown in Fig. 2. Based on Fig. 3, a dropping height of 240 mm has been used in this study to achieve a soil density of 13.5 kN/m^3. The dropping height has been maintained by lifting the dropping cone a distance equals to the thickness of the poured soil layer. After filling the container with soil to the required height, the soil surface has been leveled and excessive soil has been removed.

A hydraulic jack with a maximum loading capacity of 10 tons has been mounted on the loading frame as shown in Fig. 3. This jack has been used for installing the pile groups into the soil to the required embedded depth as well as applying the embankment loads which have been monitored using a load cell mounted on the cylindrical steel shaft. Two pile groups of (2×1) have been installed.

The first pile group, denoted by (LG) for axially loaded pile group, has been driven into the soil at a distance greater than 10 times the pile diameter from the walls of the steel container to eliminate the effect of the tip resistance [22]. While the second pile group, denoted by (UG) for axially unloaded pile group, has been driven into the soil at distance greater than 15 times the pile diameter from the first group to eliminate any rigid boundary effects [23]. Two dial gauges have been installed horizontally for each pile group at two different locations above the soil surface to measure the horizontal displacement of the pile group.

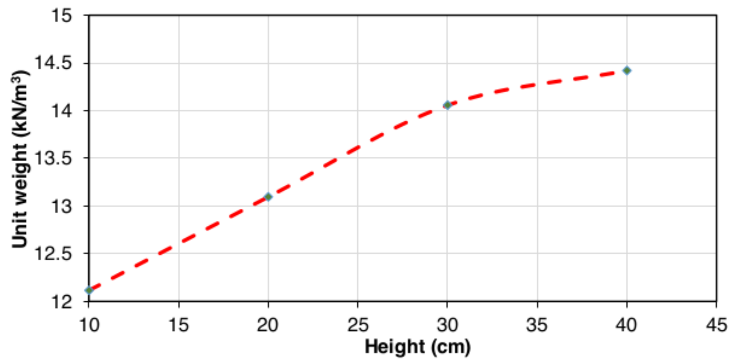

Figure 2. Effect of soil pouring height on its dry unit weight.

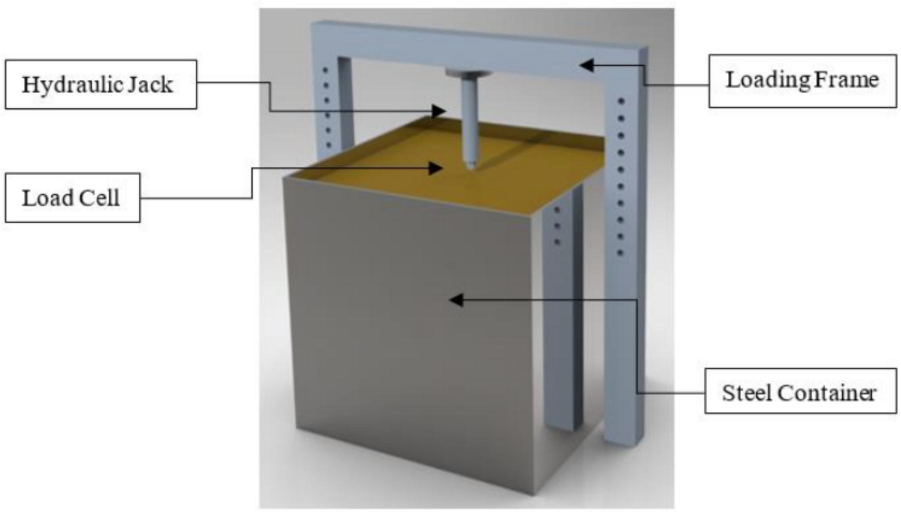

Figure 3. Schematic view of the experimental settings.

To start the experiments, the pile group (LG) has been loaded gradually up to its working axial load capacity which had been evaluated by dividing the ultimate axial load capacity by a safety factor of 2. The incremental loads have been applied by placing weights over the cap of the pile group. As a result, there has been no restriction on the head of piles and the piles have been treated as free headed piles. Then, a embankment load ranged from 10 kPa up to 60 kPa with an increment of 10 kPa has been applied at distances of 2.5D, 5D, and 10D from the pile group to simulate the effect of nearby embankments. Each embankment increment has been applied for 2 min based on the literature [24-25]. Both the dial gauge readings and the strain gauge readings have been recorded with time for each embankment load increment.

Data Analysis

The strain along the piles (ε) has been measured using the strain gauges. Using Hook's law, the flexural stress (σ) has been calculated at the strain gauge locations. Finally, the discrete bending moment (M) has been calculated using the flexural stress (see Eq. 3).

$$M = \frac{\sigma\, I_p}{D/2} = \frac{2\, E_p\, I_p}{D}\, \varepsilon \tag{3}$$

Where D is the outer diameter of the pile. To obtain a continuous response of the pile, two approaches have been reported by the literature. The first approach had been developed based on the use of a best-fit polynomial curve ranging from the 4th to the 7th order to obtain a continuous bending moment profile along the pile [26-28]. However, the drawback of this approach showed the inconsistency of the approach where multiple curves with different shapes could be used to reasonably fit the same data and, in some cases, a sudden jump in the soil reaction magnitude in the vicinity of the pile tip has been noted as reported in the literature [26-28]. The second approach had been developed based on the beam theory in which the pile responses such as the pile displacement, the pile rotation and the pile shear force profiles as well as the soil reaction profile could be derived by either differentiating or integrating the bending moment as expressed in Eq. 4 to Eq. 7 [24, 28].

$$y(z) = \int \left(\int \frac{M(z)}{E_p\, I_p}\, dz \right) dz \tag{4}$$

$$S(z) = \int \frac{M(z)}{E_p\, I_p}\, dz \tag{5}$$

$$T(z) = \frac{dM(z)}{dz} \tag{6}$$

$$P(z) = \frac{d^2 M(z)}{dz^2} \tag{7}$$

Where z is the depth measured from the soil surface downward; M(z) is the bending moment along the pile; y(z) is the pile lateral displacement; S(z) is the rotation of the axis of the pile; T(z) is the shear force along the pile and P(z) is the soil reaction along pile per unit length. In this study, a numerical integration using the trapezoidal rule has been adopted to integrate the bending moment profile. Then, the finite difference method has been used to calculate both the pile rotation and the pile deflection profiles (See Eq. 8 and Eq. 9).

$$S_i = \sum_{i=0}^{n} \frac{M_i + M_{i+1}}{2} \Delta z - S_o \tag{8}$$

$$y_i = \sum_{i=0}^{n} \frac{S_i + S_{i+1}}{2} - \Delta z - n \Delta z\, S_o + y_o \tag{9}$$

Where S_o and y_o are the integration constants of the pile rotation and the pile displacement respectively at the soil surface which has been measured directly using the dial gauges mounted at the pile head and Δz is the distance between the strain gauges. Consequently, both the shear force (T_i) and the soil reaction profiles could be obtained by using Eq. 10 and Eq. 11 respectively [25]. However, to calculate the soil reaction at any point along the pile (P_i), five bending moments should be obtained. As a result, to calculate the soil reaction (P_4), two imaginary bending moments, denoted as M_5 and M_6, have been determined to be equal to M_4 and M_3 respectively depending on the pile tip boundary conditions and the method described by Scott [29].

$$T_i = \frac{1}{2} \frac{M_{i-1} - M_{i+1}}{\Delta z} \tag{10}$$

$$P_i = \frac{1}{7} \frac{2M_{i-2} - M_{i-1} - 2M_i - M_{i+1} + 2M_{i+2}}{\Delta z^2} \tag{11}$$

Results and Discussion

The obtained results showed that the displacements at the soil surface for UG have been greater than those for LG for all cases due to the stiffening effect of the applied axial load on the latter as shown in Fig. 4. This behavior has been also observed and reported by the literature [30-32]. The increase percentages are 16, 35, and 34% for an embankment load at distances 2.5D, 5D, and 10D from the pile edge respectively. While the pile rotation at the soil surface has decreased by (61-41) and (23-70) % for LG and UG respectively as the distance from the embankment to the pile edge increased from 2.5D to 10D due to the rigid behavior of the pile groups as shown in Fig. 5.

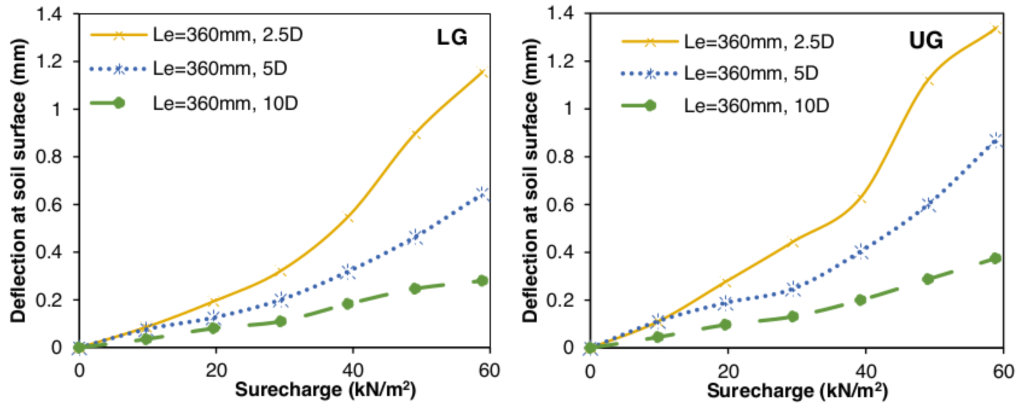

Figure 4. Displacement at soil surface of rigid piles group.

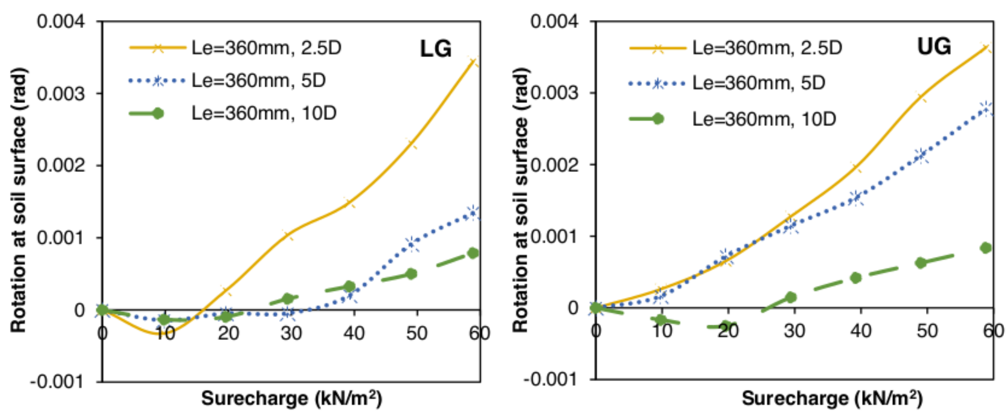

Figure 5. Rotation at soil surface of rigid piles group.

For the bending moment along the pile, the results showed that as the distance between the pile group and the embankment increased, the effect of the axial loads on the pile group decreased as shown in Fig. 6. For an embankment distance of 5D, the maximum bending moment has been found to be the same for both LG and UG. While for 10D distance of embankment, the maximum bending moment for LG has been found to be greater than the one for UG by 33%. However, for the case where a 2.5D embankment distance has been used, the maximum bending moment for LG has found to be less than the one for UG by 67% due to the stiffening effect induced by the applied axial loads on LG.

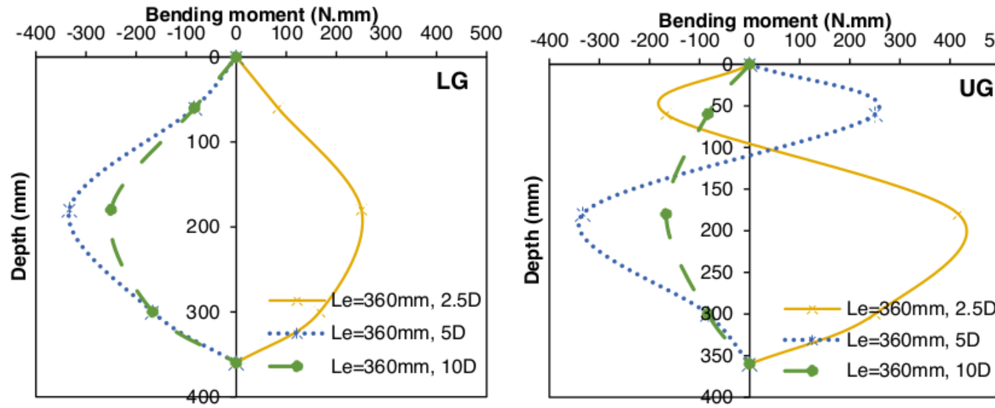

Figure 6. Bending moment profiles of rigid piles group.

Based on the pile displacement profiles, the results showed that the maximum pile displacement decreased as the distance between the embankment and the pile edge increased as shown in Fig. 7. Moreover, the application of the axial load on LG has reduced its maximum displacement when compared to UG. The results showed that UG pile head has deflected greater than that for LG by 205, 51, and 26% as the distance between the embankment and the pile edge increased from 2.5D up to 10D respectively.

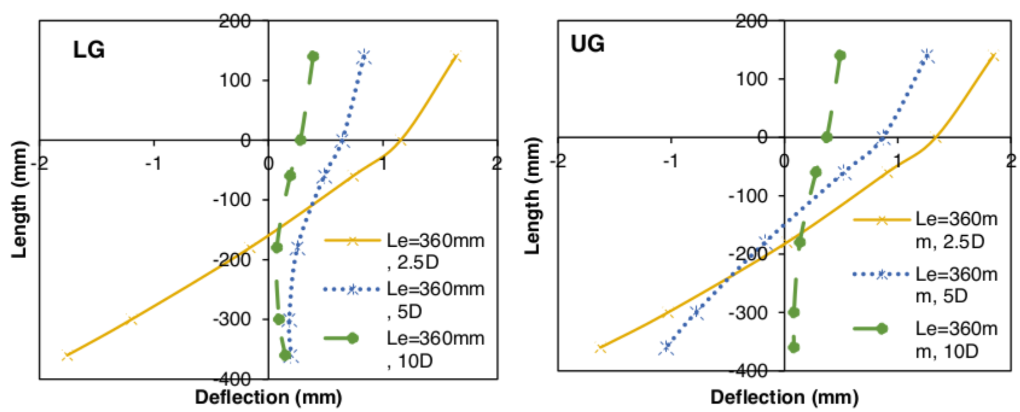

Figure 7. Deflection profiles of rigid piles group.

The results of pile rotation profiles showed that the maximum pile rotation decreased as the distance between the embankment and the pile edge increased as shown in Fig. 8. These reductions are (129 and 4) % for LG and (51 and 129) % for UG as the embankment distance increased from 2.5D to 10D respectively. In addition, the application of axial load on LG has reduced its maximum rotation when compared to UG. The results showed that the maximum pile rotation for UG has been greater than that for LG by 7, 281, and 51% as the distance between the embankment and the pile edge increased from 2.5D up to 10D respectively. For the shear forces along the pile, the results showed that the maximum shear forces for LG decreased as the distance between the pile group and the embankment increased, while the maximum shear force for UG has increased by 20% then decreased by 150% as the embankment distance increased from 2.5D to 10D respectively as shown in Fig. 9. For LG, these reductions have been found to be (225 and 25) % as the embankment distance increased from 2.5D up to 10D respectively. Furthermore, the maximum shear force for UG has found to be greater than that for LG by (25 and 220) % as the embankment distance increased from 2.5D to 5D due to the stiffening effect of the applied axial loads in LG. However, the maximum shear force for LG has found to be larger than that for UG by 25% when the embankment distance was 10 D.

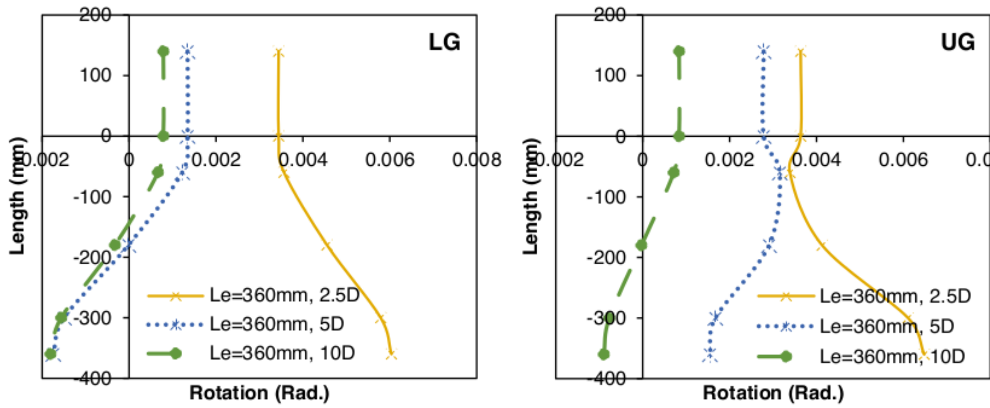

Figure 8. Rotation profiles of rigid piles group.

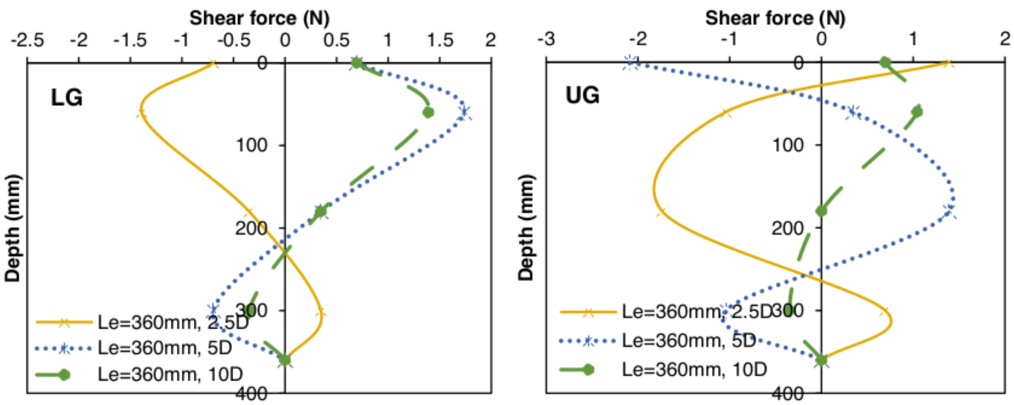

Figure 9. Shear force profiles of rigid piles group.

Finally, the results of soil reaction profiles showed that the maximum soil reaction has increased at the beginning by (200 and 20) % for both LG and UG respectively as the distance between the embankment and the pile edge increased from 2.5D to 5D. Then, the maximum shear force has decreased by (40 and 80) % for both LG and UG respectively as the embankment distance increased from 5D to 10D as shown in Fig. 10. It was found that the negative sign for the soil reaction has indicated the soil movement. While the positive sign has indicated the soil resistance to any movement.

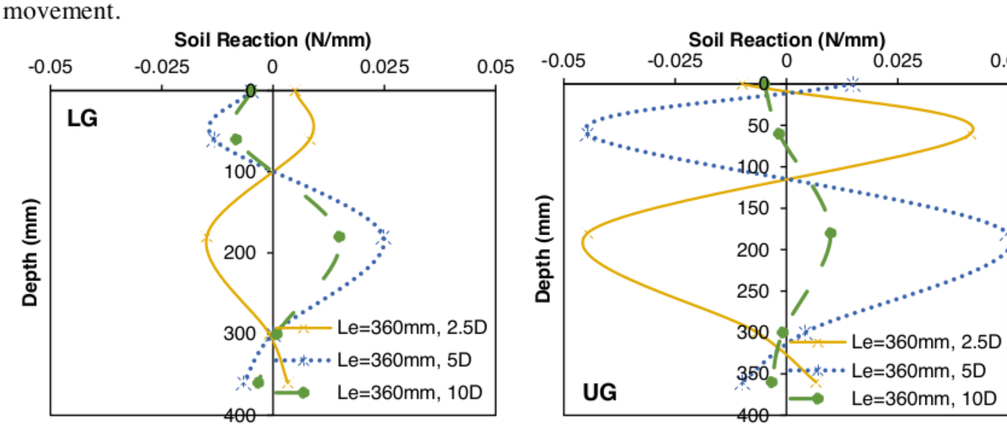

Figure 10. Soil reaction profiles of rigid piles group.

CONCLUSIONS

Based on the obtained results, the following conclusions can be made:

- The displacements at the soil surface for UG have been greater than those for LG for all cases due to the stiffening effect of the applied axial load on the latter.
- The results showed that as the distance between the pile group and the embankment increased, the effect of the axial loads on the pile group decreased on the bending moment along the pile.
- The maximum pile displacement and maximum pile rotation are decreased as the distance between the embankment and the pile edge increased.
- The maximum shear force has increased for both pile groups as the distance between the pile edge and the embankment increased from 2.5D to 5D. However, as the embankment distance has continued to be increased up to 10D, the maximum shear force has decreased for both pile groups.
- The maximum soil reaction has increased for both pile groups as the distance between the pile edge and the embankment increased from 2.5D to 5D. However, as the embankment distance has continued to be increased up to 10D, the maximum soil reaction has decreased for both pile groups due to the reduction in the soil pressure imposed by the embankment.
- The shear forces along the pile have been found to be directly related to the soil reaction along the pile.

References

[1] R. Salgado, D. Basu and M. Prezzi, Analysis of laterally loaded piles in multilayered soil deposits, Joint Transportation Research Program. Paper 330 (2008).

[2] W. G. K. Fleming, A new method for single pile settlement for prediction and analysis, Geotechnique. 42(3) (1992) 411–425.

[3] A. Ercan, Behaviour of pile groups under lateral loads, M.Sc. Thesis, Civil Engineering Department, Middle East Technical University, 2010.

[4] W. G. K. Fleming, A. J. Weltman, M. F. Randolph and W. K. Elson, Piling engineering, Taylor and Francis, London and New York, 2008.

[5] D. Beer, Piles Subjected to static lateral loads, Doctoral dissertation, Gent Royal Institute for Soil Mechanics, 1977.

[6] H. Qin, Response of pile foundations due to lateral force and soil movements, Ph.D. Thesis, Griffith University, School of Engineering, 2010.

[7] M. K. Kelesoglu, and S. F. Cinicioglu, Free-field measurements to disclose lateral reaction mechanism of piles subjected to soil movements, Journal Geotechnical and Geoenvironmental Engineering. 136(2) (2009) 331-343.

[8] Yuan, B., Chen, R., Teng, J., Peng, T., & Feng, Z., *Effect of passive pile on 3D ground deformation and on active pile response*, The Scientific World Journal, 2014.

[9] M. Zhao, D. Liu, L. Zhang and C. Jiang, 3D finite element analysis on pile-soil interaction of passive pile group, J. Cent. South Univ. Technol. 15(2008) 75-80.

[10] C. R. Zhang, M. S. Huang and F. Y. Liang, Lateral responses of piles due to excavation-induced soil movements, Geotechnical Aspects of Underground Construction in Soft Ground – Ng, Huang & Liu (eds)© 2009 Taylor & Francis Group, London, 2009.

[11] C. O. Ersoy and S. Yildirim, Experimental investigation of piles behavior subjected to lateral soil movement, Teknik Dergi. 25(4) (2014) 6867-6888.

[12] S. F. Ibrahim and M. K. Hatem, Behavior of model group piles subjected to lateral soil movement in sand, International Journal of GEOMATE, 14(44) (2018) 33-38.

[13] M. O. Karkush, A. N. Aljorany and G. S. Jaffar, Behavior of passive single pile in sandy soil, IOP Conference Series: Materials Science and Engineering, 737(1) (2020) p.012106.

[14] M. O. Karkush and G. S. Jaffar, Simulation the Behavior of Passive Rigid Pile in Sandy Soil, J. Eng. Technol. Sci., 52(4) (2020) 449-467.

[15] M. O. Karkush, G. S. Jaffar and O. K. Al-Kubaisi, Evaluating the Performance of Flexible Passive Pile Group in Cohesionless Soil Under the Effect of a Nearby Embankment. Lecture Notes in Civil Engineering, 112 (2020) 1-12.

[16] G. F. Ren, G. M. Xu, X. W. Gu, Z. Y. Cai, B. X. Shi and A. Z. Chen, Centrifuge modelling for lateral pile-soil pressure on passive part of pile group with platform, In Physical Modelling in Geotechnics, 1 (2018) 583-587.

[17] M. O. Karkush and Z. A. Kareem, Investigation the impacts of fuel oil contamination on the behaviour of passive piles group in clayey soils, European Journal of Environmental and Civil Engineering, (2018) 1-17.

[18] M. O. Karkush and Z. A. Kareem, Behavior of passive pile foundation in clayey soil contaminated with fuel oil, KSCE Journal of Civil Engineering, 23(1) (2019) 110-119.

[19] American Society for Testing and materials, Annual book of ASTM standards: soil and rock, ASTM, Philadelphia, PA, 2003.

[20] British Standards BS 1377., Methods of Testing for Civil Engineering Purpose, British Standards Institution, London, 1976.

[21] H. G. Poulos and E. H. Davies, Pile foundation analysis and design, Wiley, New York, N.Y, 1980.

[22] M. D. Bolton, M. W. Gui, J. Garnerier, J. F. Corte, G. Bagge, J. Laue and R. Renzi, Centrifuge cone penetration tests in sand, ASCE, 49(4) (1999) 543-552.

[23] H. Kishida, The ultimate bearing capacity of pipe piles in sand, Proceedings of the 3rd Asian Regional Conference of Soil Mechanics and Foundation Engineering, 1 (1967) 196-199.

[24] O. K. Ismael, Evaluating the Behavior of Laterally Loaded Piles under a Scoured Condition by Model Tests, Master Thesis, University of Kansas, 2014.

[25] S. N. Levachev, V. G. Fedorovsky, S. V. Kurillo and Y. M. Kolesnikov, Piles in hydrotechnical engineering, Taylor and Francis, 2002.

[26] S. M. Springman, Lateral loading on piles due to simulated embankment construction, Unpublished doctoral dissertation, Cambridge University, England, 1989.

[27] M. F. Bransby and S. M. Springman, Centrifuge modeling of pile groups adjacent to embankment loads, Soils and Foundations, Japanese Geotechnical Society, 37(2) (1997) 39–49.

[28] D. P. Stewart, Lateral loading of piled bridge abutments due to embankment construction, Unpublished doctoral dissertation, University of Western Australia, Australia, 1992.

[29] R. F. Scott, Foundation analysis, Prentice-Hall, Englewood Cliffs, NJ, 1981.

[30] E. H. Ghee, The response of axially loaded piles subjected to lateral soil movements, Doctoral dissertation, Griffith University, Gold Coast, Australia, 2010.

[31] W. D. Guo and H. Y. Qin, Thrust and bending moment of rigid piles subjected to moving soil, Canadian Geotechnical Journal, 47(2) (2010) 180-196.

[32] M. Samanta, R. Bhowmik and P. Mohanty, Analysis of pile group subjected to embankment induced soil movement, Proceedings of Indian Geotechnical Conference, Roorkee, 2013.

Rf

ORIGINALITY REPORT

8%	3%	4%	2%
SIMILARITY INDEX	INTERNET SOURCES	PUBLICATIONS	STUDENT PAPERS

PRIMARY SOURCES

1	Submitted to University of Baghdad Student Paper	2%
2	www.geomatejournal.com Internet Source	1%
3	D. Su, J.H. Li. "Three-dimensional finite element study of a single pile response to multidirectional lateral loadings incorporating the simplified state-dependent dilatancy model", Computers and Geotechnics, 2013 Publication	1%
4	Liang, F, C Zhang, and M Huang. "Lateral responses of piles due to excavation-induced soil movements", Geotechnical Aspects of Underground Construction in Soft Ground Proceedings of the 6th International Symposium (IS-Shanghai 2008), 2008. Publication	1%
5	nagoya.repo.nii.ac.jp Internet Source	1%
6	vsip.info Internet Source	1%

7	Zhe Li, Zhenguo Zhu, Lulu Liu, Lei Sun. "Distributions of earth pressure and soil resistance on full buried single-row anti-sliding piles in loess slopes in northern Shaanxi based on in-situ model testing", Bulletin of Engineering Geology and the Environment, 2022 Publication	1%
8	Jie Han. "Chapter 2 Behavior of Laterally-Loaded Piles Under Scoured Conditions at Bridges", Springer Science and Business Media LLC, 2022 Publication	1%

Exclude quotes	On	Exclude matches	< 1%
Exclude bibliography	On		